nature neuroscience

A supramodal accumulation-to-bound signal that determines perceptual decisions in humans

Redmond G O'Connell[1], Paul M Dockree[1] & Simon P Kelly[2]

In theoretical accounts of perceptual decision-making, a decision variable integrates noisy sensory evidence and determines action through a boundary-crossing criterion. Signals bearing these very properties have been characterized in single neurons in monkeys, but have yet to be directly identified in humans. Using a gradual target detection task, we isolated a freely evolving decision variable signal in human subjects that exhibited every aspect of the dynamics observed in its single-neuron counterparts. This signal could be continuously tracked in parallel with fully dissociable sensory encoding and motor preparation signals, and could be systematically perturbed mid-flight during decision formation. Furthermore, we found that the signal was completely domain general: it exhibited the same decision-predictive dynamics regardless of sensory modality and stimulus features and tracked cumulative evidence even in the absence of overt action. These findings provide a uniquely clear view on the neural determinants of simple perceptual decisions in humans.

Understanding how the brain can make reliable perceptual judgments despite imperfect sensory information has become a central theme of neuroscience. Almost all theoretical accounts of this process invoke two essential ingredients: the momentary encoding of sensory information necessary for the decision (evidence) and the sequential integration of evidence into a decision variable suitable for driving action. A decision variable grows monotonically with the likelihood that an emerging decision is the correct one and determines behavior through the imposition of a boundary-crossing decision criterion[1–4]. In recent years, ground-breaking single-cell recording studies in monkeys have successfully identified neuronal signals that explicitly encode these ingredients, leading to a dramatic growth of interest in the area. Sensory evidence signals have been identified that both encode relevant stimulus parameters and substantially bear on an animal's perceptual judgments independently of the sensory input[5–7]. In addition, signals resembling decision variables have been identified in brain areas involved in planning the operant actions used to indicate perceptual decisions, which build as a function of cumulative sensory evidence and exhibit a threshold effect for commitment that precisely accounts for the timing and accuracy of decisions[8–10].

The advances made in monkey neurophysiology have given rise to a strong imperative to identify sensory evidence and decision variable signals in the human brain. Success on this front not only holds promise for more mechanistically principled investigations of clinical brain disorders, but may open the door to basic research studies of higher level aspects of decision-making that are more amenable to investigation or that may even be uniquely expressed in humans[11]. However, the technical limitations of electrophysiological and functional imaging methods, such as poor spatial or temporal resolution, have rendered this a considerable challenge.

Thus far, human brain activations have been described that either correlate with parameters derived from a hypothetical decision process[12–14] or discriminate between conditions hypothesized to influence a theoretical decision variable such as difficulty[15–17]. However, no study has directly demonstrated and characterized a freely evolving signal that directly represents the decision process itself. We designed a decision-making task that allowed us to isolate the neural signatures of sensory evidence and evidence accumulation directly, without reliance on assumptions and with the bare minimum of signal processing. These electrophysiological signals exhibited every aspect of the dynamics observed in their single-neuron counterparts in terms of their inter-relationship and prediction of both the timing and accuracy of behavior. Furthermore, we found for the first time, to the best of our knowledge, the existence of an evidence-accumulating decision process that is fully domain general, exhibiting the same decision-predictive dynamics regardless of sensory modality and stimulus features, and strongly evident even in the absence of overt action.

Our task design includes four essential components. First, participants were required to detect intermittent changes in a single feature of a continuously presented stimulus. By rapidly flickering the critical sensory feature, an independent and continuous neural read-out of the momentary sensory input to the decision process could be captured in steady-state evoked responses. Second, the feature changes defining a target occurred smoothly and gradually. Human electrophysiology tasks typically involve sudden-onset, discrete stimuli that evoke a complex spatio-temporal pattern of scalp signals whose individual dynamics cannot be reliably ascertained without elaborate signal transformations[13]. The use of gradual targets eliminated transient sensory-evoked signals from the standard event-related potential, thereby offering a clear view on neural decision formation over longer timescales. Third, by using manual button-push as the operant response, we were able to continuously track the preparatory activity of contralateral pre-motor structures during decision formation via limb movement–selective

[1]Trinity College Institute of Neuroscience and School of Psychology, Trinity College Dublin, Dublin, Ireland. [2]Department of Biomedical Engineering, City College of the City University of New York, New York, New York, USA. Correspondence should be addressed to S.P.K. (skelly2@ccny.cuny.edu).

Received 24 April; accepted 24 September; published online 28 October 2012; doi:10.1038/nn.3248

beta-band (16–30 Hz) activity[18,19]. Finally, whereas almost all decision-making tasks have been divided into discrete trials with obvious or predictable evidence onset, ours was performed continuously in long, uninterrupted blocks with infrequent and unpredictable target onsets. This feature enabled investigation of the neural determinants of decision formation before as well as during target presentation, providing insight into the effects of fluctuating task engagement characteristic of natural human decision-making. A further advantage of our approach is that it is readily transferable to a range of sensory modalities, allowing us to establish the generality of human decision mechanisms.

RESULTS

We recorded 128-channel electroencephalographic data from human participants performing several versions of our continuous gradual-target detection task. In the initial version, participants continuously viewed a persistent flickering annulus for gradual contrast reductions that occurred intermittently in each of eight 4-min blocks (**Fig. 1a**). Participants made a right-handed button press the moment they were certain that the stimulus was fading. We tracked the basic sensory encoding of contrast over time by measuring the amplitude of the occipital steady-state visual-evoked potential (SSVEP)[20], driven by the on-off flickering of the stimulus at 21.25 Hz. On target onset, contrast linearly dropped from the inter-target baseline level of 65% to 35% over the course of 1.6 s, with the result that targets were very rarely missed, but were detected at highly variable latencies (mean detection accuracy, 98% ± 2.8; mean reaction time, 1,310 ms ± 160; mean intra-subject reaction time variability (s.d.), 612 ms ± 65; mean false alarms, 1.1 per block ± 1.3; **Fig. 1b**).

Neural signatures of sensory evidence and its integration

As predicted, the sensory-specific SSVEP, the motor-selective left-hemisphere beta (LHB) and the broad-band event-related potential (ERP) each underwent gradual changes on the timescale of the target contrast reduction (**Fig. 1c**). Standard ERP analysis, which simply consists of trial averaging and baseline subtraction, revealed a single, robust centro-parietal positivity (CPP) that increased steadily with incoming evidence and peaked at the time of response execution. Crucially, the use of gradual targets successfully eliminated

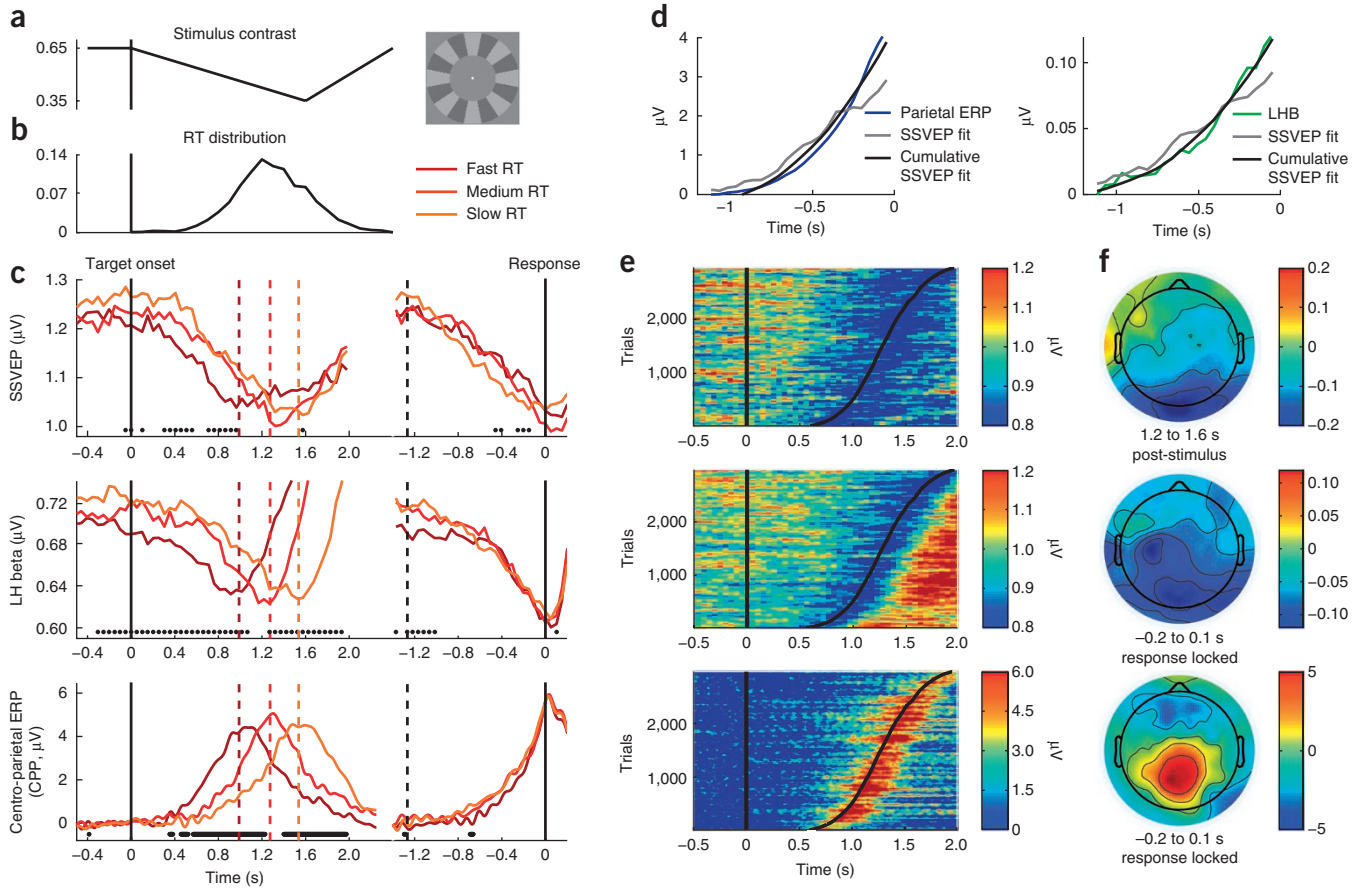

Figure 1 Distinct sensory evidence and decision signals observed during gradual target detection. (**a**) Target contrast reduction time course. (**b**) Grand-average reaction time (RT) distribution (19 subjects). Single trials were sorted by reaction time and divided into three equal-sized bins. (**c**) Neural signals undergoing gradual changes on the timescale of the physical contrast change, aligned to stimulus onset (left) and response (right). Vertical dashed lines denote mean reaction time. Markers running along the bottom of each plot indicate time points at which a linear regression of signal amplitude onto reaction time reached significance ($P < 0.05$). (**d**) The cumulative sum of SSVEP divergence from baseline provided a better fit for the dynamics of the LHB and CPP signals than the raw SSVEP amplitude. To facilitate visualization of the comparison, we baseline-subtracted and inverted SSVEP amplitude. LHB was transformed for each participant so that it reflected the percentage decrease from baseline, then inverted. (**e**) Single-trial surface plots showing the temporal relationship between each neural signal (normalized relative to each individual's baseline average) and target detection latency (curved black line). Single-trial SSVEP, LHB and CPP signals were pooled across participants, sorted by reaction time and smoothed over bins of 50 trials with a Gaussian-weighted moving average using the EEGLAB toolbox[38]. The latency of action execution was closely tied to that of the two decision signals, but was less closely related to the sensory evidence signal. (**f**) Signal scalp topographies, all with pretarget baseline subtracted. Color bars in **e** and **f** represent amplitudes.

sensory-evoked deflections from the ERP trace, making it possible to finely trace the evolution of the CPP from its onset to its peak.

To establish the dynamics of the three signals and their relationship to the timing of decision report, we split each participant's reaction time distribution into equal-sized fast, medium and slow reaction time bins and plotted the grand average signal time courses aligned to both the target onset and action execution for each bin (**Fig. 1c**). The SSVEP signal exhibited a crucial hallmark of true sensory evidence, defined as the perceptual quantity feeding directly into the decision process; its amplitude not only followed the decreasing trend of physical stimulus contrast, but also strongly predicted the timing of action independently of sensory input (that is, despite identical sensory input on all targets).

Both the LHB and the CPP signals also covaried with reaction time. Unlike the linearly decreasing SSVEP, however, the build-up rates of the LHB and CPP increased over time, indicating that they were not simply tracking the sensory evidence itself, but were instead indexing its temporal integration. To test the integration hypothesis, we performed separate regressions for each participant to fit the response-locked LHB and CPP with the SSVEP divergence from baseline and its cumulative sum, beginning 1.2 s before response time (**Fig. 1d**). The r^2 statistic for the regression on CPP increased from 63 ± 27% to 85 ± 26% when we used cumulative rather than raw SSVEP divergence (t test, $t_{18} = 4.0$, $P = 0.0009$). For LHB, r^2 increased from 53 ± 23% to 67 ± 25% ($t_{18} = 3.4$, $P = 0.003$). Thus, LHB and CPP exhibit the first predicted characteristic of the theoretical decision variable, temporal integration of sensory evidence.

The second essential characteristic of a decision variable is that the time of commitment and action execution is determined by its amplitude reaching a threshold or criterion level. Consistent with this, the response-aligned LHB and CPP waveforms (**Fig. 1c**,**e**) reached a fixed amplitude irrespective of reaction time. Furthermore, trial-to-trial variance in amplitude measured just before response initiation was significantly lower than a permutation distribution derived by randomly reassigning reaction times to trials for LHB and the CPP (both $P < 0.0001$), but not the SSVEP ($P = 0.14$, see Online Methods). An additional linear regression analysis indicated that the peak latency of LHB, CPP and SSVEP signals accounted for 85%, 90% and 20% of the variance in reaction time, respectively (all $P < 0.001$, see Online Methods). Thus, the LHB and CPP signals were better predictors of reaction time than the sensory evidence signal itself and were related to response time via a boundary-crossing criterion. The scalp distributions of the SSVEP, LHB and CPP signals are shown in **Figure 1f**.

Decision signals determine perception

To establish the connection between LHB and/or CPP and target detection accuracy, we asked a different set of participants to complete an alternate task version in which targets were presented at five randomly interleaved levels of difficulty determined by the duration of the stimulus contrast drop (**Fig. 2a**). Accuracy improved steadily as a function of contrast drop duration, with almost no detection of the hardest targets and near perfect performance on the easiest targets (**Fig. 2b**). The LHB and CPP signals markedly diverged for 'hit' compared with 'miss' trials, despite identical physical stimulation in the two cases (**Fig. 2c**). We quantified the reliability with which the single-trial amplitude of the decision signals predicted detection accuracy (hits versus misses) using a receiver operating characteristic (ROC) analysis[21] conducted at each time point in the target epoch. The ROC analysis was focused on targets at the intermediate difficulty level because the proportion of hits and misses was roughly equal on these trials (52.8 ± 18.9%). Significant deviations in classification accuracy from chance levels were determined via a permutation test (1,000 iterations with random trial reassignment conserving individual hit and miss proportions). This ROC analysis revealed strong performance-predictive activity in both LHB and CPP emerging soon after target onset and steadily increasing across the target epoch, indicating that larger amplitudes were associated with higher detection probability (**Fig. 2d**). Both signals achieved significant performance classification >600 ms before the average reaction time.

The false alarm rate was slightly higher on this version of the task (1.86 ± 1.3 per block), which allowed us to conduct a separate analysis of these events. We found that false alarms were preceded by reliable build-up in LHB and CPP (**Fig. 2c**), suggesting that the decision process was occasionally susceptible to type I error resulting from an excessive accumulation of internal, sensory noise. The LHB and CPP signals differed, however, in the extent to which their amplitudes differentiated between correct detections and false alarms. Separate ANOVAs on amplitude in an 80-ms window centered on response time, with five levels of response type (correct hits at each of the four lowest levels of

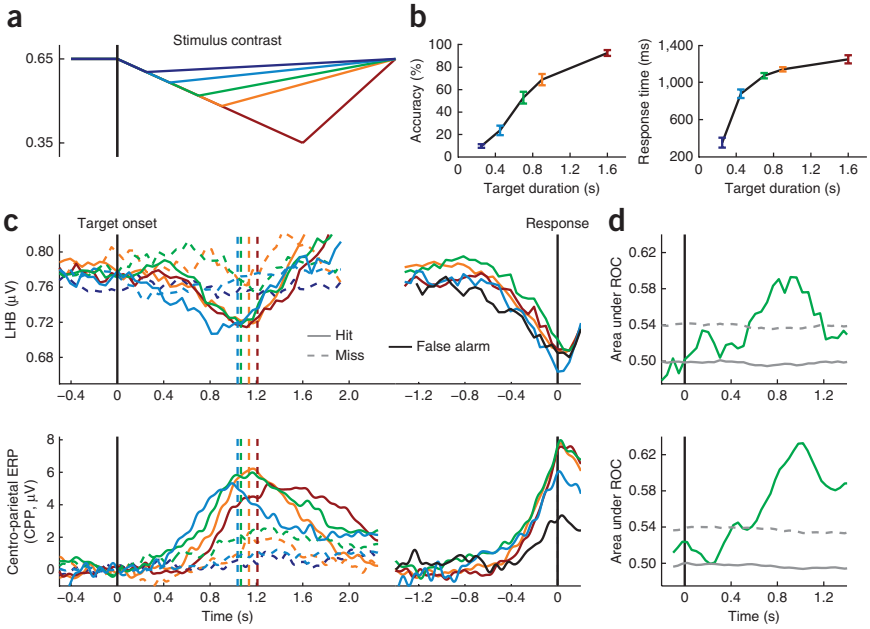

Figure 2 Decision signals determine the probability of target detection. (**a**) Contrast reduction time course of the five target-detection difficulty levels. (**b**) Detection accuracy across the 11 subjects decreased and reaction time increased as a function of target difficulty (error bars represent s.e.m.). (**c**) LHB and CPP signals for hits versus misses at each difficulty level, aligned to stimulus (left) and response onset (right). Vertical dashed lines denote mean reaction time. There were insufficient trials for analysis of hits at the hardest difficulty level and misses at the easiest level. (**d**) Time course of performance-predictive activity estimated as the area under the ROC curve. Permutation mean and significance threshold (1.96 s.d.) are marked as solid and dashed gray lines, respectively.

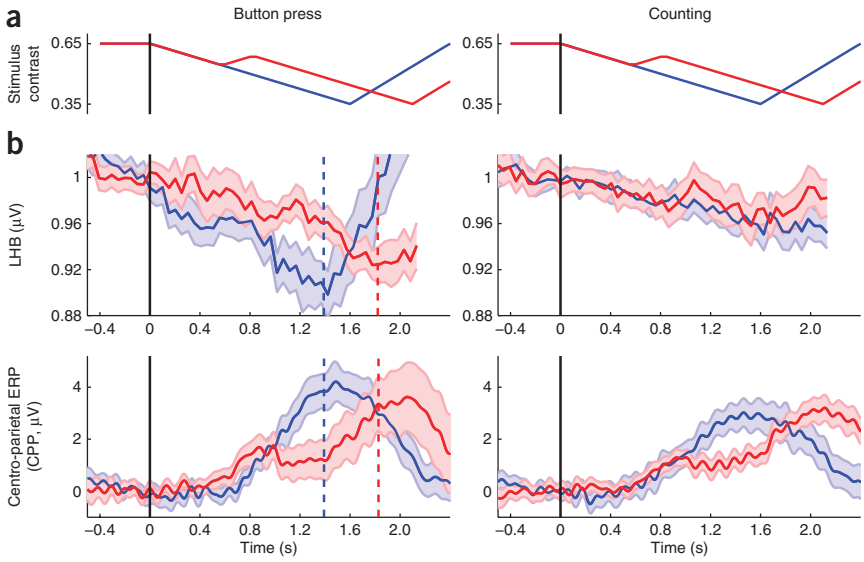

Figure 3 The CPP decision signal closely tracks incoming sensory evidence with temporal precision irrespective of action requirement. (**a**) Time course of the two different target types (regular in blue and perturbed in red). (**b**) LHB and CPP traces for the button press (left) and mental counting (right) conditions (18 subjects). Vertical dashed lines indicate mean reaction time. To reduce the influence of inter-individual variability on LHB, we normalized the single-trial traces relative to the mean baseline amplitude in each subject's average waveform. Only CPP tracked accumulating sensory evidence in both conditions.

target difficulty plus false alarms), indicated a significant main effect of response type for CPP amplitude ($F_{4,40} = 8.9$, $P < 0.0001$), but not for LHB ($F_{4,40} = 1.9$, $P = 0.14$). LHB exhibited an all-or-none relationship with responses that is characteristic of an effector-selective signal directly determining the point of motor execution (all contrasts $P > 0.1$). In contrast, false alarms were executed at significantly lower amplitudes of CPP than any correct response (all contrasts $P < 0.001$), suggesting that this signal has a more central intermediary role in regulating the translation of sensation into action.

CPP amplitude on detection of the second most difficult target level was also significantly reduced relative to the easier targets ($P < 0.01$). This may be accounted for by increased trial-to-trial variability in the distance to bound in this task, in which the evidence and detection probability randomly varied from target to target. This would have the result that hits on the most difficult targets occur only when the distance to criterion is low by chance. In addition, the peak latency of the CPP was inversely related to target difficulty ($F_{3,30} = 5.6$, $P < 0.01$; linear contrast, $P < 0.05$). This can be explained by the fact that the more difficult targets impose a shorter deadline on detection; thus, trials having an early accumulator onset by chance more likely result in a hit.

Online manipulation of evidence accumulation

We next explored the sensitivity of the two decision signals to perturbations of the physical evidence. In another task version, we randomly

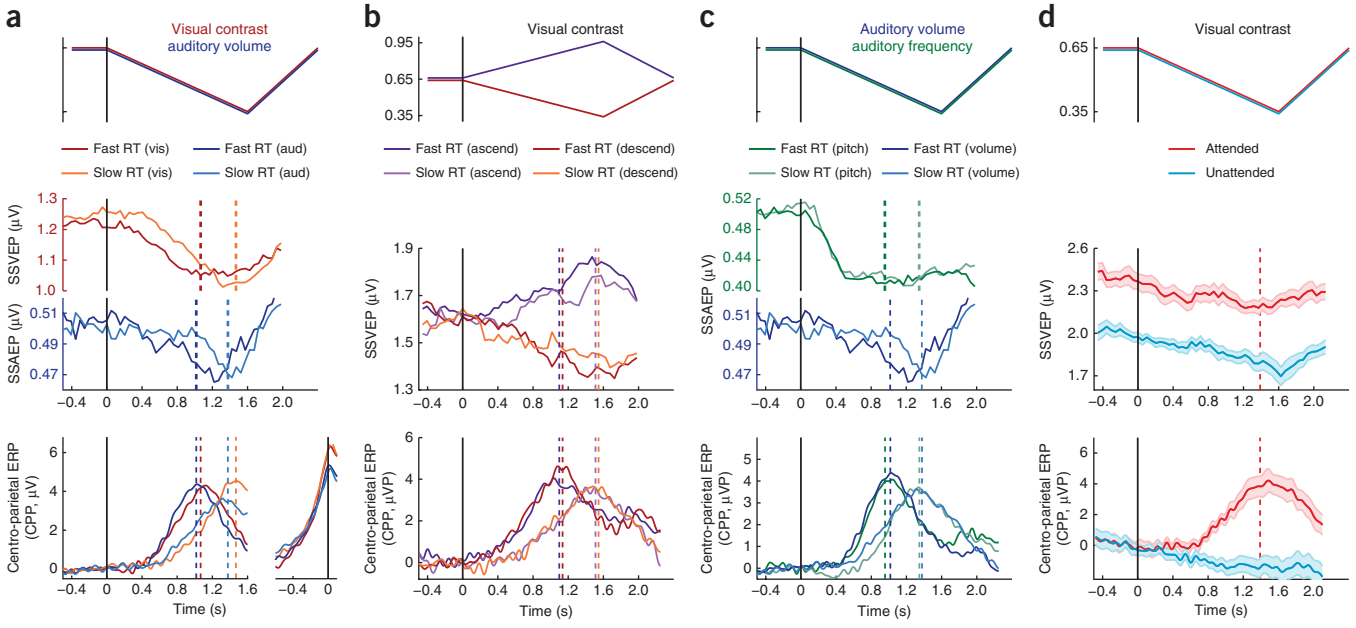

Figure 4 The CPP decision signal accumulates incoming sensory evidence irrespective of sensory modality or target feature. (**a**) Comparison of visual versus auditory versions of the gradual target task (19 subjects). Top, identical time courses were used for visual and auditory targets (defined by a linear decrease in volume). Middle, both SSVEP and SSAEP traced target emergence. Vertical dashed lines indicate mean reaction time in all panels of this figure. Bottom, CPP exhibited the same close relationship to reaction time in both modalities. (**b**) Comparison of signals when targets were defined by contrast increases versus decreases (seven subjects). Top, target contrast time courses. Middle, SSVEP showed opposite trends depending on the direction of contrast change. Bottom, CPP was unaffected by the direction of contrast change. (**c**) Comparison of signals when targets were defined by auditory volume (19 subjects) versus frequency decreases (20 subjects). Top, target time courses. Middle, by definition, the SSAEP was abolished when the frequency of the auditory envelope modulation was changed. Bottom, CPP was unaffected by the target-defining feature in the auditory domain. (**d**) Comparison of signals when targets are attended versus unattended (18 subjects). Top, contrast time courses. Middle, SSVEP traced contrast reductions even when they were unattended. Bottom, the CPP was abolished when contrast reductions were task irrelevant.

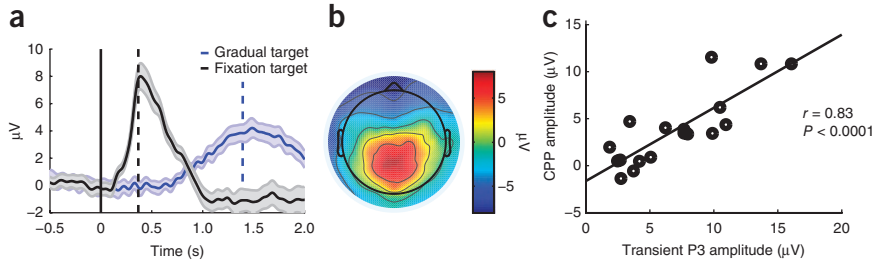

Figure 5 The CPP shares many of the characteristics of the classic P300 component. (**a**) Grand-average waveforms for P300 elicited by transient fixation targets and for the CPP elicited by gradual contrast decreases. Vertical dashed lines denote mean reaction time. Note that the smaller amplitude of the CPP versus P300 was partly a result of the substantially greater reaction time variance associated with detection of gradual targets. (**b**) The P300 had a centro-parietal scalp topography that was highly similar to that of the CPP. Color bar represents amplitude. (**c**) The peak amplitudes of the P300 and CPP were highly correlated across subjects.

interleaved the original 1.6-s contrast-drop targets with a contrast drop that was briefly interrupted at 600 ms by turning it back toward baseline for 450 ms before resuming its decline (**Fig. 3a**). Although this perturbation produced a significant delay in reaction time compared with regular targets (perturbation, 1,909 ± 148 ms; regular, 1,471 ± 131 ms; $P < 0.001$), there was no difference in accuracy (perturbation, 94.6%, ± 6.2; regular, 95.7% ± 6.1; false alarms, 0.78 ± 0.78 per block), and questioning of participants during pilot testing indicated that it was not consciously perceived.

The temporal evolution of both LHB and CPP was highly sensitive to the brief perturbation (**Fig. 3b**). The effect was even more prominent when averaging over a smaller subset of trials narrowly centered on the mode reaction time for each target type (1.3–1.7 s for the regular targets, 1.7–2.4 s for the perturbation targets; **Supplementary Fig. 1**), confirming that the grand average effect is a true representation of the single-trial dynamics and not an artifact of a bimodal reaction time distribution in the perturbation condition.

An abstract decision signal

To tease apart decision formation and motor preparation, we asked the same group of participants to repeat this version of the task, but eliminated the hand movement requirement. Instead, participants were instructed to mentally count the targets and to report the final tally at the end of each block. Detection accuracy for mental counting was comparable to performance in the button press condition (mean accuracy, 97 ± 2.7%). Analysis of the mental counting blocks revealed that the CPP continued to track the cumulative sensory evidence, whereas LHB did not (**Fig. 3b**).

The generality of the CPP was further investigated by varying the sensory requirements of the task. We first translated our task into the auditory domain by having participants monitor a continuous tone for targets that were defined by a gradual drop in volume. The tone was envelope-modulated at 40 Hz, driving an auditory cortical oscillation at the same frequency (steady-state auditory-evoked potential, SSAEP), which, similar to the SSVEP in previous iterations, provided a continual read-out of the encoding of sensory evidence. As expected, there was a steady drop in SSAEP amplitude as the target emerged. The CPP exhibited the same close relationship with reaction time in the auditory modality as it did in the visual (**Fig. 4a**). Further underlining its insensitivity to the specific content of sensory information, the CPP was reliably observed regardless of target feature in either the visual (contrast increases versus decreases) or auditory (frequency versus volume decreases) modalities (**Fig. 4b,c** and Online Methods).

A final key characteristic of a true decision variable is that it should only be responsive to goal-relevant sensory information. To test this, we returned to the original version of our task and introduced an additional condition in which participants ignored the annulus and instead monitored a small square at fixation for sudden transient increases in size. Gradual decreases in the contrast of the surrounding annulus, identical to those defining the target in the initial task version, continued to occur, but were rendered irrelevant. Despite lower tonic amplitude to the unattended annulus, the SSVEP still decreased over time alongside the now irrelevant contrast decrease, but, in this case, the CPP was extinguished (**Fig. 4d**).

Finally, we noted that the CPP shares all of the characteristics of the classic P300 ERP component (also referred to as P3b) that were measurable in the present context, including polarity, peak coincidence with response execution (**Fig. 5a**), topography (**Fig. 5b**) and contingency on task relevance[22]. When we compared the CPP to the conventional P300 that was elicited by the sudden-onset fixation targets in the final iteration of our task, we observed substantial across-subject correlations of amplitude ($r = 0.83$, $P < 0.0001$; **Fig. 5c**) and within-subject correlations of topography ($r = 0.44 \pm 0.17$, $P < 0.001$). It is likely that the topographical correlation underestimates the true relationship between P300 and CPP, as the sudden onset of the fixation targets and the tighter range of reaction time leaves the P300 far more susceptible to topographical distortion by sensory-evoked and motor components.

DISCUSSION

Our results open a new window onto the neural determinants of simple perceptual decisions in humans by isolating discrete, freely evolving neural signatures of sensory evidence encoding, decision formation and motor preparation in the human brain. These signals could be continuously monitored with a minimum of signal processing and with sufficient temporal resolution to allow their individual dynamics to be observed and systematically perturbed mid-flight during decision formation, which was previously only possible with single-neuron recordings[23]. In so doing, our results also demonstrate that the human brain employs an abstract, supramodal representation of accrued sensory evidence that exerts a deterministic influence on perceptual reports irrespective of specific sensory or motor requirements.

Theoretical and empirical neurophysiological accounts of the decision-making process offer clear predictions regarding the properties that sensory evidence and decision signals should exhibit[2,4]. To date, the vast majority of human studies have identified sensory evidence signals only on the basis of their sensitivity to relevant physical stimulus changes. This is problematic because a given sensory input can elicit signals that vary with physical content, but that do not necessarily feed into the decision process. By vastly simplifying the perceptual requirements of our task such that the relevant physical information was limited to a single persistent perceptual feature, we were able to capture a precise and continuous neural read-out of its momentary encoding in early sensory cortex. Critically, we found that trial-to-trial variability of these sensory signals predicted reaction time even when physical evidence was held constant. This observation is noteworthy given that, in drift diffusion models, response time variability is typically explained by within-trial variability of noisy evidence samples[4].

Here, the requirement for continuous monitoring over periods of several minutes is likely to have accentuated the influence of trial-to-trial attentional fluctuations on the sensory evidence signal, in comparison with the discrete trial designs used in most perceptual decision-making studies.

The defining feature of a decision variable is that its time course should build as a cumulative function of sensory evidence and determine behavior via a boundary-crossing criterion. We identified two distinct signals that shared these exact characteristics. Both LHB and CPP time courses corresponded to the cumulative sum of the sensory evidence signal and exhibited a threshold effect for commitment that precisely accounted for the perceptual reports of our participants. Build-up of the two signals was observed even when participants failed to make a response or when they falsely identified a target, confirming that they are not merely an antecedent of response execution, but instead reflect a more central detection process. Despite minimal signal processing, single trial LHB and CPP measurements achieved performance classification accuracy levels that are very similar to those obtained when single-unit signals are used to predict speeded perceptual detections in monkeys[24]. They are also markedly high given the temporal variability of short-lived decision signal peaks in our reaction time task as compared with the sustained signal elevation observed in tasks incorporating post-decision delays to response[19]. Finally, both the LHB and CPP were highly sensitive to systematic perturbation of the physical evidence during decision formation, demonstrating the tight dynamic coupling between perceptual and decision processes in the human brain.

By systematically manipulating the sensory and motor requirements of our detection task, we found that the CPP represents a previously unknown class of decision signal that accumulates evidence and determines subsequent action regardless of the sensory modality or the feature comprising the evidence, and we observed this even in the absence of overt action. The close relationship between premotor activity and behavior observed in animal studies has given rise to the dominant view that decisions are formed in an intentional framework; that is, directly in effector-specific motor planning signals[2]. The LHB measured in our study and in others[19] likely represents the same class of decision variable. However, when the need for an overt target detection response was removed in our task, the LHB ceased to encode a decision variable, indicating that this effector-specific signal does not have a general role in decision formation. Recent studies in monkeys have used tasks in which the direction of the movement needed to indicate a decision is undetermined during evidence accrual, revealing that subpopulations of LIP and superior colliculus neurons continue to exhibit decision-related activity that distinguishes categorical alternatives[25–27]. However, the accumulation-to-threshold relationship between neuronal firing rates and behavior has only been reported when stimulus-response mappings are fixed. Given that real-life decisions must be flexibly based on a diverse range of sensations and expressed through a diverse repertoire of actions, it stands to reason that domain-general decision variables exist in the brain that trace the build-up of decision certainty in a way that is invariant to the specific content of sensory or motor processing. Recent fMRI studies have pinpointed locations in the human brain where such signals may reside[11], but the limited temporal resolution of this technique has precluded verification of the critical decision-predictive properties that define a decision variable. To the best of our knowledge, the CPP represents the first conclusive evidence of a discrete signal that encodes a domain-general decision variable.

Such abstract signals may have been overlooked in animal research as a result of the reliance on recordings from a circumscribed set of premotor regions, but it is also possible that the neural circuitry governing perceptual decisions is fundamentally different in monkeys and humans. The evolution of an abstract decision mechanism that is functionally separated from motor effector systems could account for the greater flexibility of human behavior[28]. The fact that the CPP was invoked for elementary perceptual detections that entailed simple, reflexive movements suggests that, for humans at least, domain-general decision variables are a fundamental feature of decision-making.

The use of a continuous performance task made it possible to explore neural determinants of decision-making in the inter-target interval. Despite the fact that physical contrast was held constant, SSVEP and LHB were subject to substantial fluctuations, such that lower pre-target levels were associated with faster reaction time (**Fig. 1c**). This indicates that, in temporally uncertain continuous monitoring contexts, faster reaction times occur partly as a result of spontaneous changes in the momentary perception of sensory evidence (SSVEP) and/or in preparatory motor activity (LHB) straying toward execution threshold. Our task can therefore elucidate the mechanisms by which fluctuations in task engagement occurring in situations of low motivation and/or attention contribute to poorly timed or incorrect decisions[29], a facet of behavior that is almost exclusively amenable to investigations in humans.

Finally, it is interesting to note the strong similarities between the CPP and the classic P300. The P300 has been intensively studied for over four decades and has been observed in a multitude of task contexts and discriminating a range of clinical conditions[30]. Although progress was initially made in relating the P300 to specific neural computations in the framework of signal detection theory[31,32], there has been little consensus regarding its precise functional role. A major point of disagreement has been whether the P300 reflects neural processes occurring before[33,34] or after[22,35] a perceptual decision has been formed. If the CPP is indeed equivalent to the P300, our results indicate that the P300 represents the formation of the decision itself, determining behavior via a boundary-crossing criterion. The starting level of the accumulation process would be expected to vary as a function of priors, which would account for the famous sensitivity of the P300 amplitude to stimulus probability[4,36,37].

In conclusion, our results indicate that it is possible to continuously monitor independent sensory evidence, decision variable and motor preparation signals in human subjects. Our study offers a powerful new approach to the analysis of human electrophysiology that paves the way for a more mechanistically principled understanding of sensorimotor transformations in the normal and pathological brain.

METHODS

Methods and any associated references are available in the online version of the paper.

Note: Supplementary information is available in the online version of the paper.

ACKNOWLEDGMENTS

The authors thank S. Hillyard, I. Robertson, M. Bellgrove, E. Lalor and J. Balsters for helpful comments, and P. Collins, E. Lacey, C. Devine and D. Allen for their assistance with data collection. This work was supported by an Irish Research Council for Science Engineering and Technology EMPOWER fellowship (R.G.O.).

AUTHOR CONTRIBUTIONS

The study was jointly conceived by R.G.O., P.M.D. and S.P.K. The experiments and tasks were designed by R.G.O. and S.P.K. S.P.K. programmed the tasks and R.G.O. collected the data. R.G.O. and S.P.K. analyzed the data and wrote the manuscript.

COMPETING FINANCIAL INTERESTS

The authors declare no competing financial interests.

Published online at http://www.nature.com/doifinder/10.1038/nn.3248.
Reprints and permissions information is available online at http://www.nature.com/reprints/index.html.

1. Smith, P.L. & Vickers, D. The accumulator model of two-choice discrimination. *J. Math. Psychol.* **32**, 135–168 (1988).
2. Gold, J.I. & Shadlen, M.N. The neural basis of decision making. *Annu. Rev. Neurosci.* **30**, 535–574 (2007).
3. Hanes, D.P. & Schall, J.D. Neural control of voluntary movement initiation. *Science* **274**, 427–430 (1996).
4. Smith, P.L. & Ratcliff, R. Psychology and neurobiology of simple decisions. *Trends Neurosci.* **27**, 161–168 (2004).
5. Britten, K.H., Newsome, W.T., Shadlen, M.N., Celebrini, S. & Movshon, J.A. A relationship between behavioral choice and the visual responses of neurons in macaque MT. *Vis. Neurosci.* **13**, 87–100 (1996).
6. Parker, A.J. & Newsome, W.T. Sense and the single neuron: probing the physiology of perception. *Annu. Rev. Neurosci.* **21**, 227–277 (1998).
7. Romo, R. & Salinas, E. Touch and go: decision-making mechanisms in somatosensation. *Annu. Rev. Neurosci.* **24**, 107–137 (2001).
8. Kiani, R. & Shadlen, M.N. Representation of confidence associated with a decision by neurons in the parietal cortex. *Science* **324**, 759–764 (2009).
9. Kiani, R., Hanks, T.D. & Shadlen, M.N. Bounded integration in parietal cortex underlies decisions even when viewing duration is dictated by the environment. *J. Neurosci.* **28**, 3017–3029 (2008).
10. Shadlen, M.N. & Newsome, W.T. Neural basis of a perceptual decision in the parietal cortex (area LIP) of the rhesus monkey. *J. Neurophysiol.* **86**, 1916–1936 (2001).
11. Heekeren, H.R., Marrett, S. & Ungerleider, L.G. The neural systems that mediate human perceptual decision making. *Nat. Rev. Neurosci.* **9**, 467–479 (2008).
12. Philiastides, M.G., Ratcliff, R. & Sajda, P. Neural representation of task difficulty and decision making during perceptual categorization: a timing diagram. *J. Neurosci.* **26**, 8965–8975 (2006).
13. Ratcliff, R., Philiastides, M.G. & Sajda, P. Quality of evidence for perceptual decision making is indexed by trial-to-trial variability of the EEG. *Proc. Natl. Acad. Sci. USA* **106**, 6539–6544 (2009).
14. Hunt, L.T. *et al.* Mechanisms underlying cortical activity during value-guided choice. *Nat. Neurosci.* **15**, 470–476 (2012).
15. Heekeren, H.R., Marrett, S., Bandettini, P.A. & Ungerleider, L.G. A general mechanism for perceptual decision-making in the human brain. *Nature* **431**, 859–862 (2004).
16. Tosoni, A., Galati, G., Romani, G.L. & Corbetta, M. Sensory-motor mechanisms in human parietal cortex underlie abritrary visual decisions. *Nat. Neurosci.* **11**, 1446–1453 (2008).
17. Ho, T.C., Brown, S. & Serences, J.T. Domain general mechanisms of perceptual decision making in human cortex. *J. Neurosci.* **29**, 8675–8687 (2009).
18. Pfurtscheller, G. & Lopes da Silva, F.J. Event-related EEG/MEG synchronization and desynchronization: basic principles. *Clin. Neurophysiol.* **110**, 1842–1857 (1999).
19. Donner, T.H., Siegel, M., Fries, P. & Engel, A.K. Buildup of choice-predictive activity in human motor cortex during perceptual decision making. *Curr. Biol.* **19**, 1581–1585 (2009).
20. Di Russo, F. *et al.* Spatiotemporal analysis of the cortical sources of the steady-state visual evoked potential. *Hum. Brain Mapp.* **28**, 323–334 (2007).
21. Green, D.M. & Swets, J.A. *Signal Detection Theory and Psychophysics* (Wiley, New York, 1966).
22. Nieuwenhuis, S., Aston-Jones, G. & Cohen, J.D. Decision making, the P3 and the locus coeruleus–norepinephrine system. *Psychol. Bull.* **131**, 510–532 (2005).
23. Huk, A.C. & Shadlen, M.N. Neural activity in macaque parietal cortex reflects temporal integration of visual motion signals during perceptual decision making. *J. Neurosci.* **25**, 10420–10436 (2005).
24. Cook, E.P. & Maunsell, J.H. Dynamics of neuronal responses in macaque MT and VIP during motion detection. *Nat. Neurosci.* **5**, 985–994 (2002).
25. Bennur, S. & Gold, J.I. Distinct representations of a perceptual decision and the associated oculomotor plan in the monkey lateral intraparietal area. *J. Neurosci.* **31**, 913–921 (2011).
26. Horwitz, G.D., Batista, A.P. & Newsome, W.T. Representation of an abstract perceptual decision in macaque superior colliculus. *J. Neurophysiol.* **91**, 2281–2296 (2004).
27. Fitzgerald, J.K., Freedman, D. & Assad, J. Generalized associative representations in parietal cortex. *Nat. Neurosci.* **14**, 1075–1079 (2011).
28. Rorie, A.E. & Newsome, W.T. A general mechanism for decision-making in the human brain. *Trends Cogn. Sci.* **9**, 41–43 (2005).
29. O'Connell, R.G. *et al.* Uncovering the neural signature of lapsing attention: electrophysiological signals predict errors up to 20 s before they occur. *J. Neurosci.* **29**, 8604–8611 (2009).
30. Polich, J. & Criado, J.R. Neuropsychology and neuropharmacology of P3a and P3b. *Int. J. Psychophysiol.* **60**, 172–185 (2006).
31. Woods, D.L., Hillyard, S.A., Courchesne, E. & Galambos, R. Electrophysiological signs of split-second decision-making. *Science* **207**, 655–657 (1980).
32. Hillyard, S.A., Squires, K.C., Bauer, J.W. & Lindsay, P.H. Evoked potential correlates of auditory signal detection. *Science* **172**, 1357–1360 (1971).
33. Kok, A. On the utility of P3 amplitude as a measure of processing capacity. *Psychophysiology* **38**, 557–577 (2001).
34. Verleger, R., Jaskowski, P. & Wascher, E. Evidence for an integrative role of P3b in linking reaction to perception. *J. Psychophysiol.* **19**, 165–181 (2005).
35. Donchin, E. & Coles, M.G.H. Is the P300 component a manifestation of context updating? *Brain Behav. Sci.* **11**, 357–374 (1988).
36. Kopp, B. The P300 component of the event-related brain potential and Bayes' theorem. *Cogn. Sci.* **2**, 113–125 (2007).
37. Mars, R.B. *et al.* Trial-by-trial fluctuations in the event-related electroencephalogram reflect dynamic changes in the degree of surprise. *J. Neurosci.* **28**, 12539–12545 (2008).
38. Delorme, A. & Makeig, S. EEGLAB: an open source toolbox for analysis of single-trial EEG dynamics including independent component analysis. *J. Neurosci. Methods* **134**, 9–21 (2004).

ONLINE METHODS

Participants. Participants gave written informed consent, were over the age of 18, and had normal or corrected-to-normal vision, no history of psychiatric diagnosis or head injury, and no sensitivity to flickering light. Procedures were approved by the School of Psychology, Trinity College Dublin ethical review board in accordance with the Declaration of Helsinki.

Task procedures. Tests were performed in a dark sound-attenuated room while seated 50 cm from the monitor. All visual stimuli were presented on a gray background and participants were instructed to fixate on a centrally presented 5 × 5–pixel white square. Unless otherwise stated, visual stimuli were presented on a 55-cm LCD monitor with 120-Hz frame rate. Auditory stimuli were delivered via headphones. Prior to recording, participants completed a short practice block of eight targets, and rested between blocks thereafter.

Task version 1: fixed visual contrast decrease and auditory volume decrease. The first task version was administered to 24 participants, of which five were excluded from analysis because of excessive artifacts (>50% trial loss), leaving a final sample of 19 participants (five females, one left-handed, mean age of 20.4 ± 4). Stimuli were presented on a 51-cm CRT monitor operating an 85-Hz refresh rate.

Participants continuously monitored an annular flickering (21.25 Hz) pattern stimulus (inner radius = 1.14°, outer radius = 2.29°) for intermittent targets defined by linear contrast changes from 65 to 35% over 1.6 s. The annular pattern consisted of alternating light and dark radial segments, with two cycles per quadrant. The inter-target interval was randomly 4, 7.2 or 10.4 s. Participants performed eight blocks, each lasting 4 min and containing 25 targets. Participants were instructed to avoid guessing and make a right index finger mouse button press as soon as they were certain that the annulus was fading.

To enable investigation of the domain generality of our decision signals, participants also performed eight 4-min blocks of an auditory analog of the visual task in which they monitored a continuous 500-Hz, 70-dB tone, envelope-modulated at 40 Hz, for targets that were defined by a linear reduction in volume reaching 30% at 1.6 s, matching targets in the visual condition. The sensory modality of the task alternated block by block, and the condition that was performed first was counter-balanced across participants. The visual stimulus was continuously presented in parallel during the auditory detection blocks and vice versa, but the unattended stimulus in each condition was held constant at all times to ensure that it was completely irrelevant to the task at hand.

Manual responses made >150 ms into a target interval were identified as hits. Target detection responses after the physical evidence had peaked (1.6 s) were extremely rare (0.6 ± 0.8%), confirming that participants did not use the return to baseline as a cue that a target had been presented. Nevertheless, these late responses were excluded from electrophysiological analyses in all task conditions.

Task version 2: visual contrast decreases of variable duration. To establish the connection between LHB, CPP and target detection accuracy, participants monitored a 20-Hz flickering annulus (as in version 1, except inner radius = 1.14°, outer radius = 3.1°) for targets that were presented at five randomly interleaved levels of difficulty by manipulating the duration of the downward ramp in stimulus contrast. After peaking, contrast linearly increased to reach baseline level at 2.4 s post-onset for all conditions, guarding against the possibility that the return to baseline exogenously cues target appearance. This task was performed by 15 participants, two of which were excluded from analysis because they made insufficient misses (<10) to allow a comparison of hits versus misses at any single target difficulty level. A further two participants were rejected because of insufficient false alarms (<10), leaving a final sample of 11 right-handed participants (three males, mean age = 20.4 ± 4).

Participants performed 12 4-min blocks (25 targets) of the task. The hardest and easiest difficulty levels were presented less often than the intermediate difficulty levels (12.5% versus 25%), as only the latter levels were intended to be divided into hits and misses. Participants were informed that the duration, and therefore the magnitude, of stimulus fading would vary from target to target and instructed to respond as soon as they were sure that the stimulus was fading. Feedback on the percentage detection accuracy for each level of difficulty was provided after every block to promote effort maintenance.

Task version 3: perturbation of sensory evidence, manipulation of response requirements and task relevance. A single group of 20 participants performed three separate conditions. Two participants were excluded because of poor counting performance in condition 2 (detection accuracy < 2.5 s.d. below group average) leaving a final sample size of 18 (seven female, two left-handed, mean age = 22.1 ± 4.3).

To establish the sensitivity of the decision signals to perturbations of the sensory evidence, participants completed five 4-min blocks in which they monitored a 20-Hz flickering annulus (as described in task version 2) for contrast decreases and indicated detections with a speeded mouse button press (condition 1). Two different contrast-decrease time courses were randomly interleaved: regular trials that were identical to task version 1 and perturbation trials that contained contrast-direction reversals at 400 and 850 ms.

To test the extent to which the decision signals were driven by the requirement for an overt motor response, participants performed the same task as described above, but instead of using a button-push response, participants were asked to mentally count the targets and to report the final total at the end of each block (condition 2). We presented 23–27 targets (inclusive, uniform distribution) in each block.

To establish the extent to which the CPP was specifically elicited by task-relevant sensory information, participants performed two further blocks in which they were presented with the same flickering annulus, but were asked to monitor the central fixation square for transient (100 ms) increases in size from 5 to 10 pixels (condition 3). Participants were asked to indicate these fixation targets with a speeded button press. Gradual decreases in the contrast of the surrounding annulus, identical to those defining the target in conditions 1 and 2, continued to occur, but were rendered irrelevant by the task instructions. Identical inter-trial intervals intermediated between gradual changes. Fixation targets were presented at random times between the offset of an annulus contrast change and 800 ms preceding the following contrast change.

All participants completed the two blocks of condition 3 first to ensure that the contrast decreases would not capture attention. Fixation targets were detected with 100 ± 0% accuracy with an average reaction time of 362 ± 19 ms and 0.06 ± 0.24 false alarms. Thirteen of the participants completed the five blocks of conditions 1 and 2 in sequence, but with the order of conditions counter-balanced across participants. The five remaining participants alternated block by block between conditions 1 and 2. Subanalyses revealed that the results from these five were entirely consistent with those of the other 13 participants.

Task version 4: visual contrast increases versus decreases. To test the sensitivity of the CPP to changes in the target feature, we compared two conditions in which a group of seven participants (four male, one left-handed, mean age = 23.3 ± 2.3) alternated block by block between monitoring the flickering annulus for contrast increases (linear rise to 95%) versus decreases (linear drop to 35%, identical to version 1). The starting condition was counter-balanced across participants. Participants completed 3–6 blocks of each condition. On average participants detected 95.6 ± 3.8% of ascending targets with reaction time of 1,314 ± 129 ms and 1.5 ± 1.2 false alarms, and detected 96 ± 5.1% of descending targets with reaction time of 1,348 ± 153 ms, 0.75 ± 0.99 false alarms.

Task version 5: decreases in auditory frequency versus volume. To further test the generality of the CPP across target features, we administered an alternate version of the auditory task used in version 1 in which participants monitored a continuous auditory tone for a gradual decrease in frequency from 40 to 30 Hz. A 9-cm diameter circular pattern with linearly increasing contrast from 0 to 100% from center to perimeter was flickered at fixation at 21.25 Hz during auditory performance to allow direct comparison with task version 1, but, again, its contrast was held constant at all times. Visual stimuli were presented on a 51-cm CRT monitor operating a 85-Hz refresh rate.

This version was administered to 23 participants, three of which were excluded from the analysis because of excessive artifacts (>50% trial loss), leaving a final sample of 20 participants (seven female, one left-handed, mean age = 21.7 ± 3.2). On average, participants detected 95.9 ± 3.0% of auditory targets with reaction time of 1,215 ± 182 ms and 0.9 ± 0.6 false alarms. In **Figure 4**, we compare these data for frequency-decrease targets to the data of version 1 (volume decreases) to demonstrate the CPP's insensitivity to changes in auditory target feature.

doi:10.1038/nn.3248

Electroencephalogram (EEG) acquisition and analysis. Continuous EEG was acquired using an ActiveTwo system (BioSemi) from 128 scalp electrodes, digitized at 512 Hz. Eye movements were recorded using two vertical electro-oculogram (EOG) electrodes placed above and below the left eye and two horizontal EOG electrodes placed at the outer canthus of each eye. Data were analyzed in Matlab. Noisy EEG channels were interpolated using spherical spline interpolation implemented in EEGLAB[38] and EEG data were re-referenced offline to the average reference. Target epochs were extracted from 750 ms before target onset to 400 ms after peak sensory evidence. Trials were rejected if the bipolar vertical EOG signal exceeded ±200 μV at any time in the epoch or if any scalp channel exceeded 100 μV. SSVEP (21.25 or 20 Hz depending on task version), SSAEP (40 Hz) and LHB (22–30 Hz, avoiding the SSVEP frequency) were measured using the standard short-time Fourier transform with a boxcar window size fitting exactly eight cycles of the SSVEP frequency and 50-ms step size. SSVEP was averaged over seven electrodes centered on standard 10–20 site Oz. SSAEP was averaged across three midline electrodes running posteriorly from standard site Fz. LHB was averaged over three electrodes around standard left-hemisphere motor site C3. The CPP analysis consisted simply of averaging the single-trial waveforms, which were baseline-corrected relative to the 500-ms interval before target onset. CPP amplitude and latency measures were taken from the average of three electrodes centered on standard site CPz. The grand-average waveforms were low-pass filtered up to 10 Hz for display only. To test for the boundary-crossing criterion effect in our signals, we compared the trial-to-trial variance of signal amplitudes measured just before response initiation (−180 to −80 ms, ending at motor potential onset; **Supplementary Fig. 2**) to the expected value of the same variance metric computed in the case in which reaction times were randomly reassigned to trials. We tested this for LHB, CPP and SSVEP using 500 permutations for each individual subject. To account for the increased noise in the CPP measure compared with the more robust band-limited measures of LHB and SSVEP, variance values were computed for amplitude measures of each of the three signals in bins of five trials, grouped after sorting trials in order of increasing reaction time. These values were representative of the values obtained for larger bin sizes (**Supplementary Fig. 3**). A linear regression analysis was conducted to further quantify the extent to which the peak latency of each signal accounted for trial-to-trial variance in reaction time. To control for possible differences in the signal-to-noise ratios of each signal, the single-trial traces were pooled across subjects, sorted by reaction time and, through repeated iterations, averaged across bins of increasing size (1–80). Separate regression analyses were then conducted for each bin size. The reaction time variance explained increased monotonically with bin size for all three signals and the values reported in the text were taken from representative bin sizes (**Supplementary Fig. 4**).